Reprinted from the JOURNAL OF LUBRICATION TECHNOLOGY, *Vol. 99, No. 1, January 1977*

E. J. Gunter
Professor.

L. E. Barrett
Research Engineer.

P. E. Allaire
Assistant Professor.

Department of Mechanical Engineering, University of Virginia, Charlottesville, Va.

Design of Nonlinear Squeeze-Film Dampers for Aircraft Engines

This paper examines the effect of squeeze-film damper bearings on the steady state and transient unbalance response of aircraft engine rotors. The nonlinear effects of the damper are examined, and the variance of the motion due to unbalance, static pressurization, retainer springs, and rotor preload is shown. The nonlinear analysis is performed using a time-transient method incorporating a solution of the Reynolds equation at each instant in time. The analysis shows that excessive stiffness in the damper results in large journal amplitudes and transmission of bearing forces to the engine casing which greatly exceed the unbalance forces. Reduction of the total effective bearing stiffness through static pressurization and rotor preload is considered. The reduction in stiffness allows the damping generated by the bearing to be more effective in attenuating rotor forces. It is observed that in an unpressurized damper, the dynamic transmissibility will exceed unity when the unbalance eccentricity exceeds approximately 50 percent of the damper clearance for the relatively wide range of conditions examined in this study.

1 Introduction

Modern aircraft engines typically utilize rolling element bearings mounted in oil squeeze film damper bearings to attempt attenuation of vibrational amplitudes and to promote rotor stability. Linearized analyses have shown that the supports must be carefully tuned to the particular rotor system in order to improve machine performance [1–4].[1] In particular there is a range of support damping and stiffness values which will improve rotor performance. Values outside the optimum range may result in substantially worse performance than that exhibited by the rigidly supported rotor [5, 6].

This paper is concerned with the design of an oil film damper to attenuate the forces transmitted to bearing support structure and engine casing for a typical aircraft turbine engine. Nonlinear time transient techniques are used to show the ability of the damper to compensate for a suddenly applied unbalance and to reduce the steady-state motion to acceptable levels of amplitude and force transmission. Results indicate that an improperly designed damper can become overloaded, even with small amounts of unbalance, causing a force several times larger than the rotating unbalance to be transmitted to the engine structural members. In addition, experimental results illustrating this and other effects are presented.

2 Theoretical Analysis

2.1. **Reynolds Equation.** The configuration of the squeeze film damper bearing is shown in Fig. 1, where the clearance has been exaggerated. Both fixed and rotating coordinate systems are shown, and the bearing equations are derived for both systems.

The basic bearing equation is the Reynolds equation, which is derived from the Navier-Stokes equations for incompressible flow. With the proper bearing parameters the equation for the fluid film forces are derived [7]. The short bearing approximation is used since most dampers have a low L/D ratio [8].

The Reynolds equation for the short, plain journal bearing is given in both fixed coordinates by:

$$\frac{\partial}{\partial Z}\left[\frac{h^3}{6\mu}\frac{\partial P}{\partial Z}\right] = (\omega_b + \omega_j)\frac{\partial h}{\partial \theta} + 2\frac{\partial h}{\partial t} \tag{1}$$

In the fixed coordinate system the film thickness, h, is given by:

$$h = c - x\cos\theta - y\sin\theta \tag{2}$$

Substituting into equation (1) and integrating yields:

$$P(\theta, Z) = \frac{3\mu}{h^3}[Z^2 - LZ]\left[(\omega_b + \omega_j)\frac{\partial h}{\partial \theta} + 2\frac{\partial h}{\partial t}\right] \tag{3}$$

2.2. **Bearing Forces in Fixed Coordinates.** The total force components in the x and y directions are found by integrating the pressure over the entire journal surface.

For the case of the squeeze film damper where the journal and housing are constrained from rotating, ($\omega_b = \omega_j = 0$), the force expression becomes

$$\begin{Bmatrix} F_x \\ F_y \end{Bmatrix} = \frac{-\mu R L^3}{2}\int_0^{2\pi} \frac{-2(\dot{x}\cos\theta + \dot{y}\sin\theta)}{(c - x\cos\theta - y\sin\theta)^3}\begin{Bmatrix}\cos\theta \\ \sin\theta\end{Bmatrix} d\theta \tag{4}$$

[1] Numbers in brackets designate References at the end of paper.

Contributed by the Lubrication Division and presented at the Joint Lubrication Conference, Boston, Mass., October 5–7, 1976, of THE AMERICAN SOCIETY OF MECHANICAL ENGINEERS. Manuscript received by the Lubrication Division January 7, 1976; revised manuscript received March 10, 1976. Paper No. 76-Lub-25.

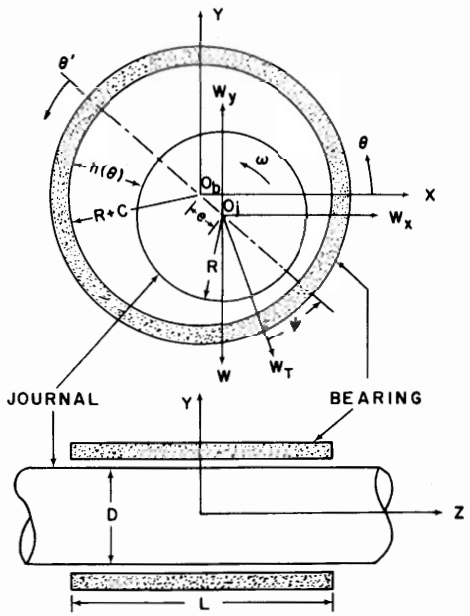

Fig. 1 Schematic of squeeze film damper bearing

The nonlinear fluid film forces are easily combined with the rotor bearing system dynamical equations providing a complete nonlinear dynamical analysis of the system. Because the bearing force equations are written in fixed Cartesian coordinates, a transformation from one coordinate system to another is not required. This is very important for conservation of computation time since the bearing pressure profile must be integrated at each time step of the system motion.

2.3. **Bearing Forces in Rotating Coordinates.** If the Reynolds equation is written in polar coordinates, it may be integrated in closed form assuming steady-state circular precession of the journal about the bearing center and no axial misalignment. The resulting equations for the bearing forces give the equivalent stiffness and damping of the bearing.

The force components are:

$$\begin{Bmatrix} F_r \\ F_\theta \end{Bmatrix} = \frac{-\mu RL^3}{c^2} \int_{\theta_1'}^{\theta_2'} \frac{(\dot{\phi}\epsilon \sin\theta' + \dot{\epsilon}\cos\theta')}{(1+\epsilon\cos\theta')^3} \begin{Bmatrix} \cos\theta' \\ \sin\theta' \end{Bmatrix} d\theta' \tag{5}$$

The limits of integration, θ_1' and θ_2', define the area over which a positive pressure profile exists and are dependent on the type of journal motion and whether or not cavitation occurs.

It is assumed that the damper is precessing in steady-state circular motion about the origin and therefore $\dot{\epsilon} = 0$.

The resulting force components are:

$$F_r = \frac{-2\mu RL^3 \epsilon\omega e}{c^3(1-\epsilon^2)^2} \tag{6}$$

and

$$F_\theta = \frac{-\mu RL^3 \pi e\omega}{2c^3(1-\epsilon^2)^{3/2}} \tag{7}$$

The force in equation (6) appears as a stiffness coefficient times a displacement acting in line of the displacement toward the bearing center. The equivalent damper stiffness is:

$$K_0 = \frac{2\mu RL^3\epsilon\omega}{c^3(1-\epsilon^2)^2} \tag{8}$$

Since the journal is precessing and not rotating, every point in the journal has a velocity equal to $e\omega$. The force in equation (7) therefore appears as a damping coefficient times a velocity acting in the direction opposite the journal motion.

The equivalent damper damping is:

$$C_0 = \frac{\mu RL^3\pi}{2c^3(1-\epsilon^2)^{3/2}} \tag{9}$$

For the uncavitated film, the components are given by:

$$F_r = 0 \tag{10}$$

$$F_\theta = \frac{-\mu RL^3\pi e\omega}{c^3(1-\epsilon^2)^{3/2}} \tag{11}$$

It is therefore evident that a complete fluid film does not produce an equivalent bearing stiffness, but doubles the damping of the cavitated film.

Although the equations for the damper characteristics were derived for a plain damper, they are applicable to other damper configurations such as those shown in Fig. 2. A damper with a circumferential oil groove and full end leakage, shown in Fig. 2(*a*), consists of two plain lands of length $L/2$. The net effect of cutting a circumferential oil groove in the damper is to decrease the hydrodynamic force and both bearing coefficients by a factor of four.

The damper represented in Fig. 2(*b*) has a circumferential oil groove and end seals to prevent end leakage. Since the hydrodynamic pressure vanishes at the center, the pressure profile is equivalent to that for a plain land without an oil groove and without end seals.

The damper equations derived in this section are summarized in Table 1. Also included in the table are the equations for pure radial squeeze motion. For this type of operation $\dot{\phi} = 0$, and it results from a purely unidirectional load on the journal. The radial and tangential force components are derived from equation (5), where only the term containing $\dot{\epsilon}$ in the integral is retained. The pressure equation is also modified to include only the $\dot{\epsilon}$ term. The maximum pressure occurs at $\theta' = \pi$ for all values of journal eccentricity. Examination of the pressure equation reveals that the hydrodynamic pressure is positive only in the region $\theta' = \pi/2$ to $3\pi/2$. These values of θ' are the limits of

Nomenclature

A = journal amplitude, e/c, DIM
c = bearing clearance, L
C_0 = equivalent bearing damping, FTL^{-1}
$C_{xx}, C_{xy}, C_{yy}, C_{yx}$ = bearing damping, FTL^{-1}
e = journal eccentricity, L
EMU, EU = ratio of unbalance eccentricity to bearing clearance, DIM
F_x = force component in x-direction, F
F_y = force component in y-direction, F
F_r = force component in radial direction, F
F_θ = force component in tangential direction, F
$FMAX$ = maximum hydrodynamic force, F
FU = force due to rotating unbalance, F
h = fluid film thickness, L
K_0 = equivalent bearing stiffness, FL^{-1}
KR, KRX, KRY = retainer spring stiffness, FL^{-1}
L = bearing length, L
m = rotor mass, FT^2L^{-1}
N = rotor speed, REV/T
P = pressure, FL^{-2}
P_a = ambient pressure, FL^{-2}
P_c = lubricant cavitation pressure, FL^{-2}
$PMAX$ = maximum hydrodynamic pressure, FL^{-2}
R = bearing radius, L
t = time, T
TRD, TD = transmissibility coefficient, $FMAX/FU$, DIM
W = weight, F
x, y, z = displacements, L
$\dot{x}, \dot{y}$ = velocities, LT^{-1}
ϵ = eccentricity ratio, e/c, DIM
$\dot{\epsilon}$ = radial velocity, T^{-1}
μ = viscosity, FTL^{-2}
θ, θ' = angular measure, rad
ϕ = phase angle, rad
$\dot{\phi}$ = journal precession rate, T^{-1}
ψ = attitude angle, rad
ω_b = angular velocity of bearing housing, T^{-1}
ω_j = angular velocity of journal, T^{-1}
ω_s = natural frequency of rotor on retainer spring $\sqrt{KR/m}$, T^{-1}

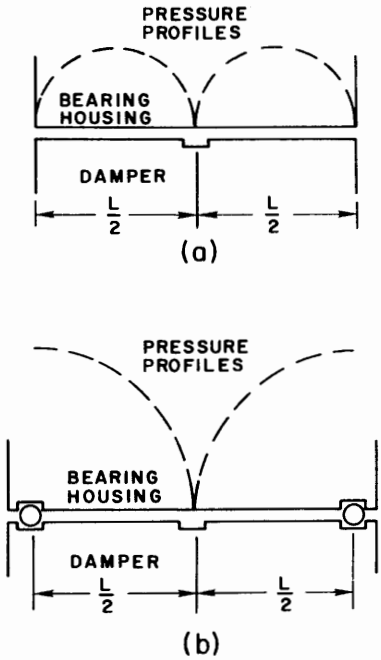

Fig. 2 Damper bearing configurations with circumferential oil supply groove with and without end seals

TYPE OF MOTION	MAXIMUM PRESSURE	EQUIVALENT STIFFNESS Ko (N/cm)	EQUIVALENT DAMPING Co (N-sec/cm)
CIRCULAR SYNCHRONOUS PRECESSION $\dot{\phi} = \omega$, $\dot{\epsilon} = 0$	$\frac{-3\mu L^2 \omega \epsilon \sin\theta_m}{2c^2(1+\epsilon\cos\theta_m)^3}$ where θ_m is given by:	$\frac{2\mu RL^3 \epsilon\omega}{c^3(1-\epsilon^2)^2}$	$\frac{\mu RL^3}{2c^3(1-\epsilon^2)^{3/2}}\pi$
CAVITATED FILM			
UNCAVITATED FILM	$(1+\epsilon\cos\theta_m)\cos\theta_m+3\epsilon\sin^2\theta_m=0$	0	$\frac{\mu RL^3}{c^3(1-\epsilon^2)^{3/2}}\pi$
PURE RADIAL SQUEEZE MOTION $\dot{\phi} = 0$, $\dot{\epsilon} \neq 0$	$\frac{-3\mu L^2 \dot{\epsilon} \cos\theta_m}{2c^2(1+\epsilon\cos\theta_m)^3}$	0	$\frac{\mu RL^3[\pi-\cos^{-1}(\epsilon)](2\epsilon^2+1)}{c^3(1-\epsilon^2)^{5/2}}$
CAVITATED FILM	$\theta_m = \pi$		
UNCAVITATED FILM		0	$\frac{\mu RL^3\pi(2\epsilon^2+1)}{c^3(1-\epsilon^2)^{5/2}}$

integration in equation (5) for the cavitated film.

The table also shows that for purely radial motion no damper stiffness is obtained in either the cavitated or uncavitated damper. Thus if this type of motion exists, retainer springs must be included to provide support flexibility.

For the case of circular damper precession, the table shows that damping of the cavitated and the uncavitated film remains essentially constant for low eccentricity ratios. As the eccentricity ratio increases above 0.4, there is a rapid increase in both stiffness and damping, and they approach infinity as ϵ approaches 1. This variation of stiffness in the cavitated film is very important. As the eccentricity becomes large, the support becomes more rigid with a corresponding increase in the rotor critical speed. If the rotor critical speed is increased above the operating speed, the phase angle between the rotor unbalance vector and amplitude vector becomes less than 90 deg. When this condition occurs, the force transmitted through the support structure will always be greater than the unbalance load. With an uncavitated film, this problem does not occur because no damper stiffness is generated. To obtain the stiffness required to stabilize a rotor, it is necessary to use retainer springs in the support bearings.

3 Application of Squeeze Damper to Gas Turbine Engine

Fig. 3(*a*) represents a typical cross section of a two-spool jet engine showing the deflected mode shapes of the stator and the gas generator rotor. In this particular application, the squeeze film damper is

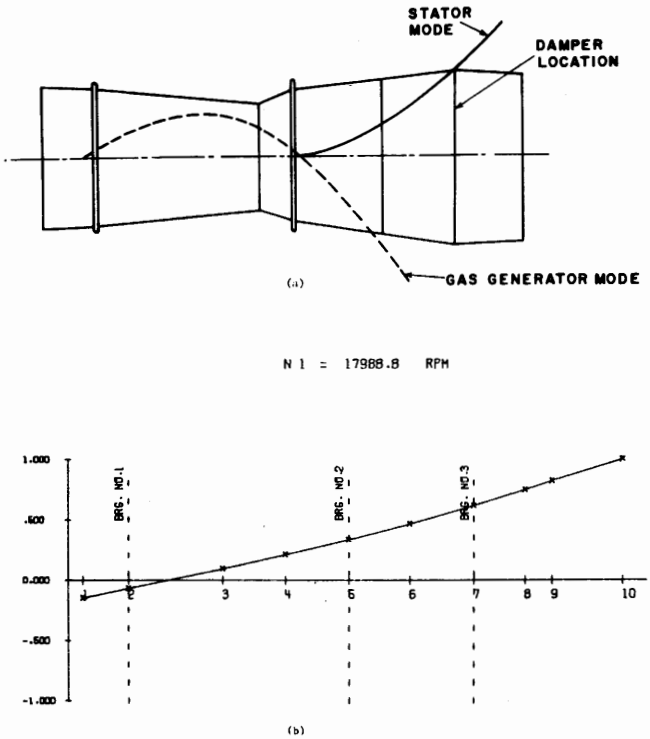

Fig. 3 Typical aircraft engine cross section and gas generator critical speed mode shape

mounted at the first stage nozzle diaphram and is used to control the amplitude of motion of the overhung generator section while passing through the first critical speed. Testing showed that under certain conditions the turbine would reach extremely high amplitude levels with certain ranges of unbalance.

3.1 **Squeeze Film Damper Stiffness and Damping Characteristics for Circular Precession.** The stiffness and damping coefficients associated with the damper employed in this engine are shown in Figs. 4(*a*) and 4(*b*). Fig. 4(*a*) represents the damping characteristics for various radial clearances versus eccentricity ratio for the turbine operating at a speed of 16,800 rpm with an effective damper length of 0.45 in. (1.14 cm). The damping curves are based on the equations shown in Table 1. For example, with a radial damper clearance of 4 mils (0.0102 cm) and an operating eccentricity ratio of 0.5, the damping generated by this configuration is only 3.5 lb-s/in. (6.13 N-s/cm). Based on a turbine weight of 73.7 lb (327.82 N) and an expected critical speed of 18,000 rpm, this value represents only 0.45 percent of critical damping. Therefore it should not be expected that a large attenuation of rotor amplitude can be accomplished with this value.

Fig. 4(*b*) represents the effective radial stiffness of the damper versus eccentricity ratio assuming synchronous orbital motion of the journal about the damper center. If the oil film in the damper cavitates, as it will unless the damper has a high oil supply pressure, the damper will produce an equivalent radial spring rate which increases rapidly with eccentricity. If the journal is operating with a circular synchronous orbit of radius 0.5 and a radial clearance of 4 mils (0.0102 cm), then the effective spring rate produced will be 4,000 lb/in. (7,004 N/cm). If the journal eccentricity ratio increases to 0.9, then the radial spring rate increases by a factor of 25, from 4,000 to over 100,000 lb/in. (7,004 to 175,118 N/cm). At this high eccentricity, however, the damping coefficient only increases by a factor of 7.5 from 3.5 to 26 lb-s/in. (6.13 to 45.53 N-s/cm). Therefore if the journal operates at eccentricity ratios greater than 0.5, the radial bearing stiffness increases at a much faster rate than the damping. This produces an undesirable effect in that it increases the effective stiffness acting on the rotor and produces a highly nonlinear rotor system.

3.2 **Nonlinear Transient Analysis of Narrow Width Damper.** The values of stiffness and damping produced in the curves were based on the assumption of circular synchronous motion. In order to investigate the complete dynamical behavior of the nonlinear damper under unidirectional loading and with or without the effects of a retainer spring rate, a nonlinear transient analysis was carried out. The theory of the nonlinear transient analysis of rotor bearing systems is given in [4, 7]. In this case, the rotor equations of motion are numerically integrated forward in time, and the squeeze film hydrodynamic forces are calculated at each time interval by an integration of the Reynolds equation. This then allows one to track the rotor motion in the damper and to determine the amplitude and forces transmitted. Fig. 5(*a*) represents the transient motion of the turbine in a squeeze film damper with a retainer spring of 123,000 lb/in. (215,395 N/cm). The rotor is released and rapidly assumes a limit cycle at an eccentricity ratio of approximately 0.95.

The unbalance of approximately 2.5 oz-in. (1.76 N/cm) represents a rotating load of 1,182 lb (5,257 N). This represents a displacement of the rotor mass center of approximately 50 percent of the bearing clearance (*EMU* = 0.5). It is seen that in this case the dynamic transmissibility is 6.2, which indicates that a maximum force of 7,331 lb (32,608 N) is transmitted through the damper, which is higher than that for a turbine mounted on a rigid support. In proper damper design, the dynamic transmissibility should be less than 1 in order to attenuate the rotating unbalance forces.

In Fig. 5(*b*) the transient motion of the rotor was simulated without a retainer spring in order to reduce the stiffness of the system. In this case it is seen that a few more cycles are required in order to achieve the steady-state circular motion of the damper, but the dynamic transmissibility (6.27) has not been improved by removing the retainer spring rate. Therefore it is seen that with this particular damper design, the small specified unbalance of only 2.5 oz-in. (1.76 N/cm) would severely overload the damper and would not result in successful attenuation of the rotor forces throughout the rotor operating speed range.

In order to reduce the effective damper stiffness the clearance was increased from 4 to 6 mils (0.0102 to 0.0152 cm). Fig. 5(*c*) shows the transient which results with the same unbalance as before (the dimensionless unbalance, *EMU*, is different because the clearance has been changed). The damper journal quickly spirals outward to form a limit cycle at an eccentricity ratio of $\epsilon = 0.95$. The dynamic transmissibility, *TRD*, indicates a force of over seven times the rotating unbalance load and peak hydrodynamic pressures over 40,000 psi (2,721 bar) are generated.

As an alternative method to reduce the damper stiffness, the damper was pressurized to a mean static pressure of 400 psi (27.2 bar) as shown in Fig. 5(*d*). The limit cycle eccentricity ratio is $\epsilon = 0.95$ and the dynamic transmissibility is 6.15. Due to the high hydrodynamic pressures generated, over 24,000 psi (1,633 bar), no realistic static pressure could be applied to significantly reduce cavitation and hence the effective damper stiffness.

If the unbalance level is reduced from *EMU* = 0.5 to 0.25, the maximum hydrodynamic pressure is reduced from over 24,000 psi (1,633 bar) to about 1,000 psi (68 bar) as shown in Fig. 6(*a*). Although this results in a reduction of the dynamic transmissibility, the whirl orbit is no longer synchronous, but appears to have a half frequency component. The nonsynchronous whirl orbit does not appear to diminish, even after 10 cycles of motion. Fig. 6(*b*) shows the effect of increasing the mean static pressure to 400 psi (27.2 bar). The dynamic

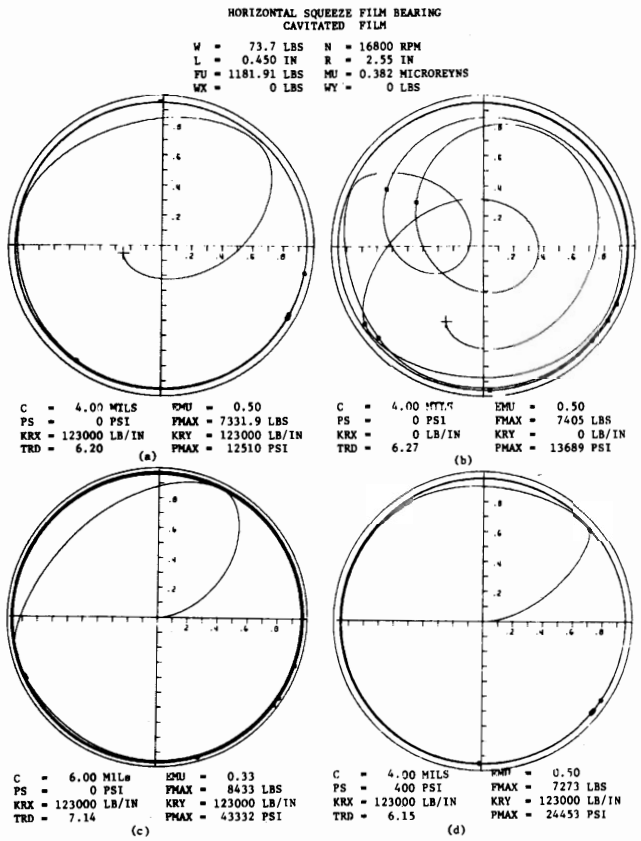

Fig. 5 Transient orbits of unbalanced rotor showing effects of variation in clearance, supply pressure, and retainer springs, *L* = 1.14 cm

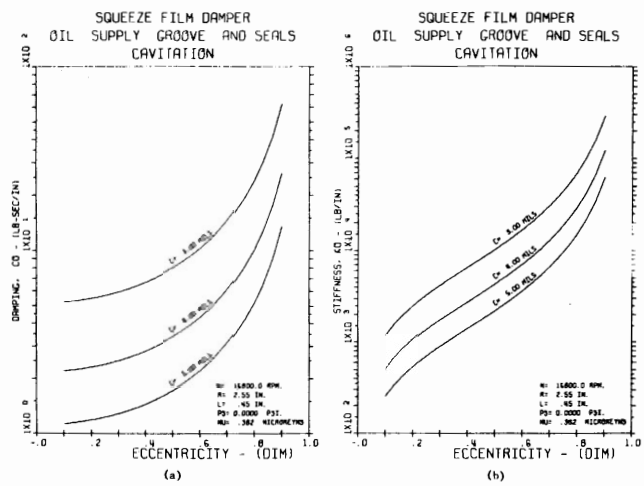

Fig. 4 Damping and stiffness coefficients for squeeze film bearing, *L* = 1.14 cm

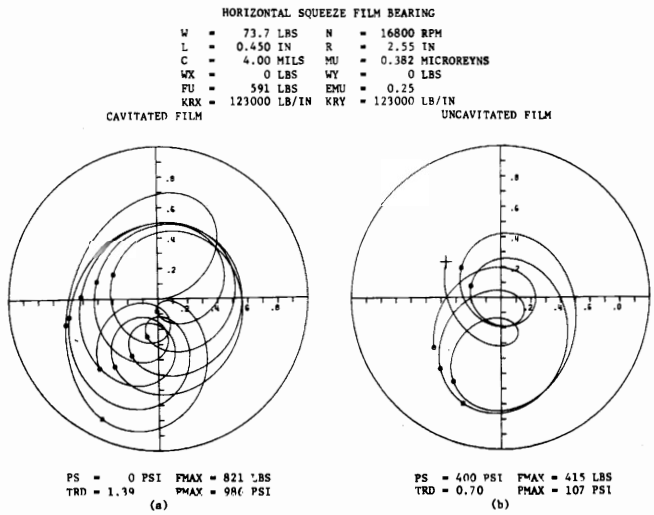

Fig. 6 Transient orbits or unbalanced rotor showing effects of supply pressure, *L* = 1.14 cm

transmissibility is reduced still further to $TRD = 0.70$ and the fluid film is fully uncavitated with peak hydrodynamic pressures of about 100 psi (6.8 bar). The whirl orbit is still nonsynchronous and the nonsynchronous component does not appear to diminish. Even though the dynamic transmissibility has been reduced for these cases, the resulting nonsynchronous whirl components are normally undesirable because of their ability to excite unstable operational modes in rotor systems.

3.3 **Approximate Estimation of Damper Characteristics From Limit Cycle Motion.** The circles on the orbit represent the timing marks for each cycle of shaft motion. From the observation of these timing marks an estimate of the change of the rotor phase angle with respect to the rotating unbalance can be determined. In Fig. 5(*a*), the phase angle change between the displacement vector and the rotating forcing function is 30 deg. From the knowledge of the rotor phase angle change and amplitude, the effective stiffness and damping characteristics of the damper may be calculated. Unless the rotor has gone through a phase angle change of approximately 120 deg, it can be shown that the dynamic transmissibility will not be below unity.

From elementary single mass theory, the equivalent stiffness and damping may be computed from the mass of the rotor and the experimentally determined rotating unbalance force, phase angle change, and amplitude as follows:

$$A = \frac{m\omega^2 EMU}{\sqrt{(K_0 - m\omega^2)^2 + (C_0\omega)^2}} \tag{12}$$

and

$$\tan\phi = \frac{C_0\omega}{K_0 - m\omega^2} \tag{13}$$

where A and ϕ are obtained from oscilloscope plots. Solving for C_0 and K_0 gives

$$C_0 = \frac{m\omega EMU}{A\sqrt{1 + \left(\frac{1}{\tan\phi}\right)^2}} \tag{14}$$

$$K_0 = \frac{C_0\omega}{\tan\phi} + m\omega^2 \tag{15}$$

For $A = 0.95$, $\phi = 30$ deg, $\omega = 1{,}759$ rad/s, and $EMU = 0.50$, the system damping and stiffness are calculated at $C_0 = 88$ lb-s/in. (154 N-s/cm) and $K_0 = 860{,}000$ lb/in. (1.506×10^6 N/cm) (see also Fig. 5(*a*)).

3.4 **Dynamic Characteristics and Transient Motion of Improved Damper With Increased Width.** Fig. 7 represents the damping and the stiffness characteristics for a damper in which the effective length has been increased from 0.45 to 0.90 in. (1.14 to 2.28 cm). In this way the effective damping for a 4 mil (0.0102 cm) clearance system can be increased without drastically increasing the damper stiffness at low eccentricities. Fig. 8(*a*) represents the rotor motion with the increased damper length and the unbalance reduced from $EMU = 0.5$ to 0.25. In this case, it is observed that the dynamic transmissibility is 0.65. Therefore the damper system has been effective in reducing the dynamic transmissibility for this particular case. In Fig. 8(*b*) the retainer spring is eliminated and the rotor is seen to also operate successfully with a dynamic transmissibility of less than 1. However, the removal of the retainer spring rate has caused an increase of the dynamic transmissibility from 0.65 to 0.8. The orbit of the rotor is not circular, but contains an internal half frequency loop. From the observations of the timing marks on Fig. 8(*a*), it is seen that the marks do not all correspond to one point or area. Therefore the motion is not purely synchronous motion, but has developed a two to one frequency component due to the nonlinear forces developed in the squeeze film damper. A two to one frequency ratio has been observed in other cases when the damper is subjected to a unidirectional loading.

Figs. 8(*c*) and 8(*d*) are similar to Fig. 6, in which the unbalance eccentricity is $EMU = 0.5$, but the damper length has been increased from 0.45 to 0.9 in. (1.14 to 2.29 cm). It can be seen in this case that either with or without the retainer spring the dynamic transmissibility

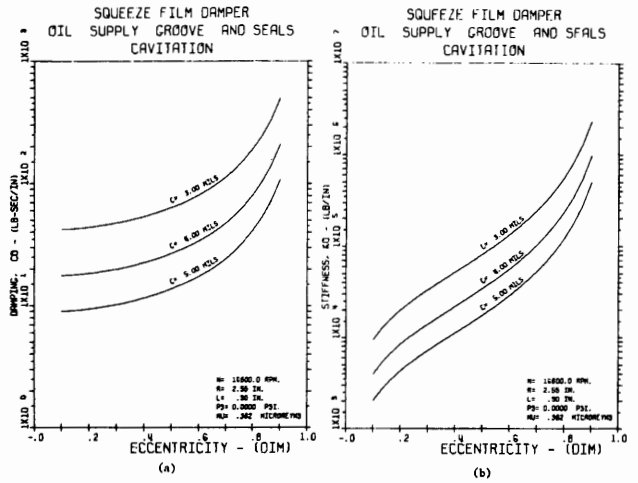

Fig. 7 Damping and stiffness coefficients for squeeze film bearing, $L = 2.28$ cm

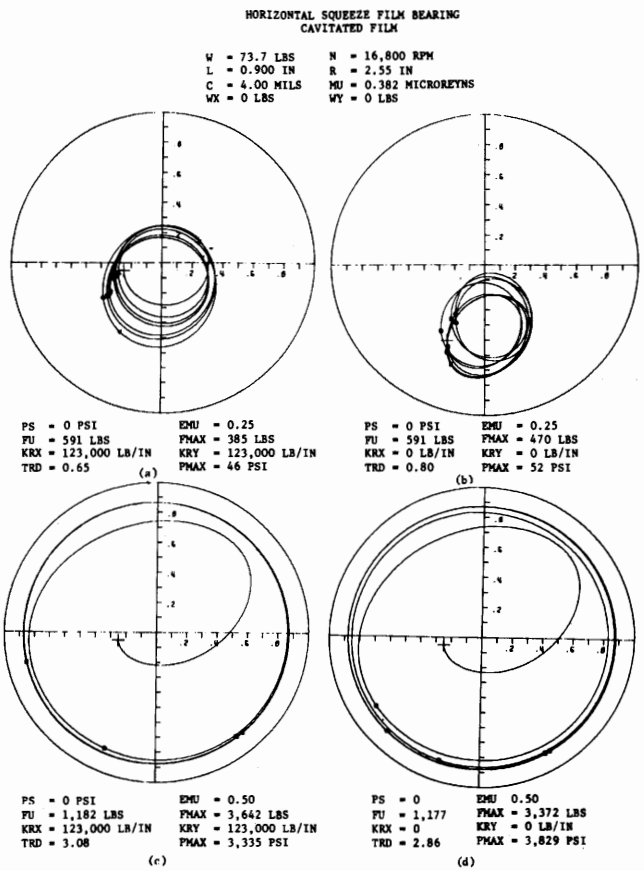

Fig. 8 Transient orbits of unbalance rotor showing effects of variation in unbalance and retainer spring, $L = 2.28$ cm

is greater than 1. In the first case with the retainer spring, the dynamic transmissibility has been reduced from 6.2 to 3.08. The elimination of the retainer spring reduces the dynamic transmissibility only slightly to 2.86. Therefore it is seen that with the level of unbalance chosen even the increased length of the damper is insufficient to cause a reduction of the dynamic transmissibility below 1.

The dynamic transmissibility greater than 1 is again caused by the fact that the damper is generating a highly nonlinear radial spring rate which causes the forces transmitted to increase rapidly with eccentricity. If the damper is pressurized to eliminate or reduce the cavitation, then the damping coefficient is increased while the effective

spring rate that the damper produces is drastically reduced. However, in this case a retainer spring rate must be employed with the system or the damper will not lift off during startup. Fig. 9(a) represents the damper with the high unbalance eccentricity of $EMU = 0.5$, but the damper has been pressurized with an oil supply pressure of 4,000 psi (272.11 bar). In reality it may not be feasible to supply such a high pressure to the damper, but what it does illustrate is that this has a dramatic effect on the dynamic transmissibility by causing a reduction of the transmissibility from 3.08 to 0.95. Even a pressure of 400 psi (27.21 bar) will eliminate the cavitation in the damper and greatly improve its performance.

In Fig. 9(a) the effect of pressurization has caused an effective reduction of the squeeze film stiffness characteristic and an increase in its effective damping. Approximate values for the squeeze damper stiffness and damping characteristics can be determined from the amplitude and phase angle of the orbital motion as before. It is important to note that this procedure can be performed experimentally from an oscilloscope picture. The journal motion is circular synchronous precession, with the origin offset from the damper center at approximately $\epsilon_0 = 0.11$. Using the value of ϵ_0, the orbit amplitude is $A = 0.62$ and the phase angle is $\phi = 157$ deg. The effective damping coefficient for the system is approximately 106 lb-s/in. (185.62 N-s/cm). If the damper were cavitated and operating with an orbital amplitude of $A = 0.62$, the damping coefficient would be 37 lb-s/in. (64.79 N-s/cm). If the film were completely uncavitated, then the damping coefficient would increase to 74 lb-s/in. (129.59 N-s/cm). However, since the journal is operating at an offset eccentricity of $\epsilon_0 = 0.11$, the effective damping has been increased from 74 to 106 lb-s/in. (129 to 185.63 N-s/cm). In the previous curves it was shown that if the damper fully cavitates, then a large radial stiffness term is generated in the film. In this case the effective stiffness is calculated to be 151,425 lb/in. (265,176 N/cm). Therefore it is seen that the pressurization of the damper has greatly reduced the damper spring rate due to hydrodynamic forces to only 27,000 lb/in. (47,282 N/cm).

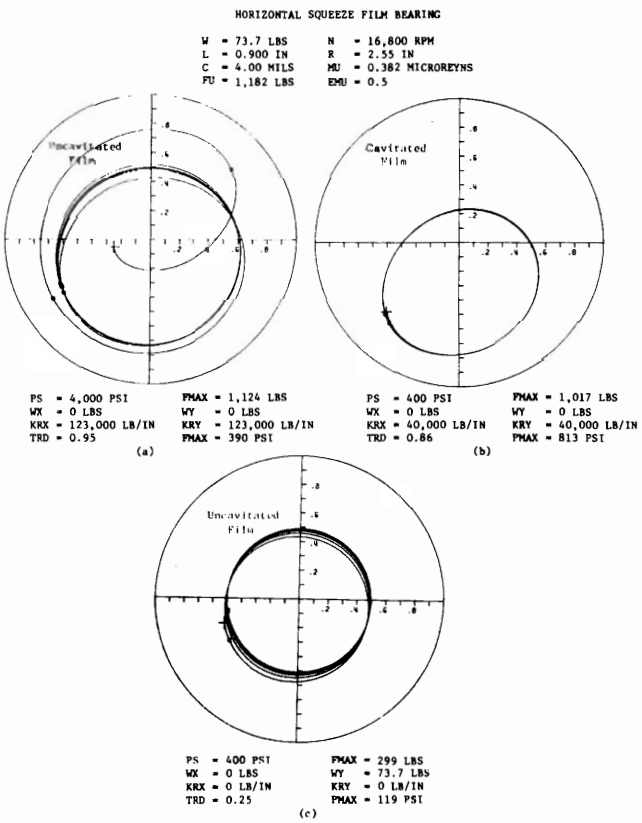

Fig. 9 Transient orbits of unbalanced rotor showing effects of cavitation, supply pressure, retainer spring, and preload. $L = 2.28$ cm

It should also be noted that if this damper were operated without a retainer spring and with full pressurization, it is unlikely that lift-off would occur.

Fig. 9(b) shows the effect of increasing the mean static pressure to 400 psi (27.21 bar) for the case shown in Fig. 9(a). The retainer spring stiffness has also been reduced to 40,000 lb/in. (70,047 N/cm). The fluid film does partially cavitate, but the reduction in effective damper stiffness has resulted in a nearly circular synchronous orbit. The dynamic transmissibility is now only 0.86. Fig. 9(c) shows the effect of eliminating the retainer spring and preloading the rotor so that it is aligned with the bearing center. This has been accomplished by applying a unidirectional load, or preload of 73.7 lb (327.82 N), to counteract the gravitational loading. The resulting limit cycle is circular and synchronous and is centered about the bearing center. In this case the fluid film does not cavitate and therefore there is no effective bearing stiffness. The rotor therefore operates at an eccentricity equal to the unbalance eccentricity, $EMU = \epsilon = 0.5$, and the dynamic transmissibility has been further reduced to $TRD = 0.25$. This damper configuration is hence highly desirable from the standpoint of force attenuation. The preload also insures that the journal will lift off during engine startup.

3.5 **Nonlinear Equilibrium Solution and Forces Transmitted for Circular Synchronous Precession.** For small displacements of the motion about the damper origin, the squeeze film characteristics may be taken as linearized stiffness and damping parameters. It is apparent both from the steady-state motion and the damper equations that for large eccentricities the damper forces are highly nonlinear and that the unbalance magnitude has a major effect on the amplitude of the steady-state orbit. Mohan and Hahn [10] have shown that there is a limit to the unbalance eccentricity at which the squeeze film damper is able to successfully operate. Fig. 10 represents the dynamic transmissibility versus speed ratio for various values of unbalance eccentricity. In order for the damper to operate successfully, the dynamic transmissibility should be less than 1. If the speed ratio (ω/ω_s) is less than approximately 1.5, the dynamic transmissibility will always be greater than 1. For the sample damper investigated, the value of ω_s represents the natural frequency of the rotor on the retainer spring rate, which is 7,700 rpm. Therefore the frequency ratio of the machine is 2.18. The transmissibility curve developed by Mohan shows that above a speed ratio of 1.5, the dynamic transmissibility for the circular synchronous motion about the origin can be kept below 1 provided the unbalance eccentricity is less than $EMU = 0.4$. Mohan also showed that with an unbalance eccentricity of 0.4, there exists the possibility of a nonlinear jump above a speed ratio of 2.7. Since the squeeze film forces are similar to a hardening spring effect, there may theoretically be three equilibrium positions of the damper in certain speed ranges. The lower amplitude of motion is the most desirable region of operation since the rotor mass center has effectively inverted and the dynamic transmissibility is less than 1. The upper solution is undesirable as the dynamic transmissibility is considerably greater than 1. The intermediate solution is unstable and the rotor motion will jump from one curve to the other. The equilibrium position that the damper will assume is dependent upon the initial or starting value of motion. Thus in those cases where $EMU = 0.5$ and cavitation occurs, the dynamic transmissibility is expected to exceed 1.

4 Experimental Rotor Motion

Fig. 11 shows the gas turbine rotor experimental amplitude versus speed as observed on a typical engine. It can be seen that the rotor amplitude builds up to a maximum value of 8 mils (9.9102 cm) as observed on the casing at 17,000 rpm and then goes through a "jump." In this engine the radial damper clearance is 4 mils (0.0102 cm). Therefore the 8 mil (0.0204 cm) peak to peak vibration observed indicates that the damper may be completely overloaded. After the jump, there is a low level of rotor motion. In this particular case, the jump is possible only because of the flexibility of the supporting structure of the damper bearing to the engine casing. The difference in jump speeds in Figs. 11(a) and 11(b) is because of a change in the support structure. Large damper motion such as this has caused

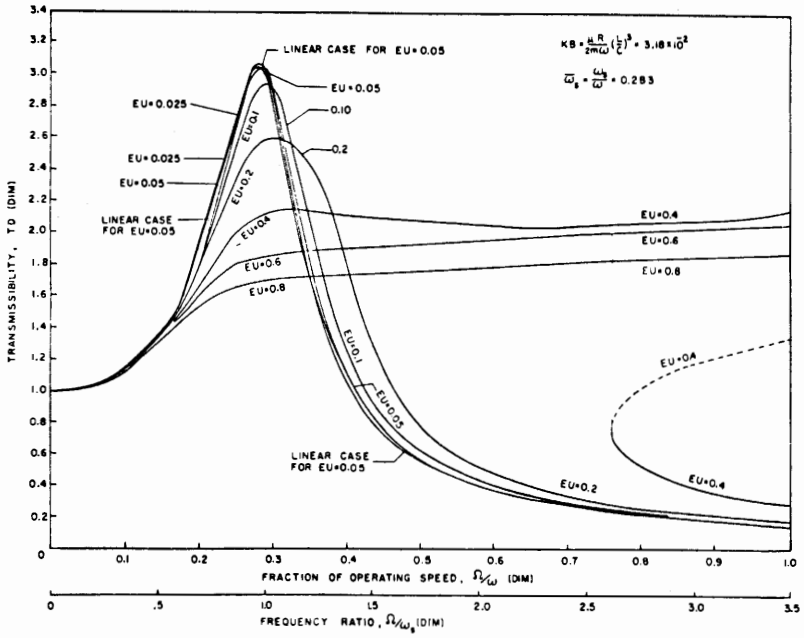

Fig. 10 Bearing force transmissibility versus rotor speed for rotor with various values of unbalance [10]

cracking of the supporting structures in the past and should be avoided. Whenever large jump phenomena such as this are observed with aircraft engines using damper supports, it is indicative that the damper bearing is overloaded. A well designed damper support system should never exhibit this type of phenomenon. If the maximum operating eccentricity is designed not to exceed $\epsilon = 0.4$, then the maximum allowable amplitude that should be observed at the damper would be 3.2 mils (0.0081 cm) peak to peak motion. Fig. 12 shows the experimental motion of the damper support system as seen on an oscilloscope with a change of rotational speed from 16,500 rpm to 17,500 rpm . In Fig. 12(*b*) the oil supply pressure is increased slightly, and it can be seen that a rapid reduction of rotor motion has occurred, indicating the rotor has passed the jump speed.

5 Conclusions

1 Squeeze film damper bearings for promotion of rotor stability and attenuation of transmitted forces must be specifically tuned for each particular rotor-bearing system. Excessive stiffness in the damper results in less effective rotor damping and increased force transmission. Thus damper bearing designs must consider methods of reducing the stiffness while retaining the required amount of damping.

2 The hydrodynamic forces in damper bearings are highly nonlinear functions of the journal operating eccentricity and velocity. If the journal undergoes circular synchronous precession about the bearing center, linearized hydrodynamic stiffness and damping coefficients may be calculated.

3 The linearized damping coefficient is relatively constant for journal eccentricities below 0.4. The linearized stiffness coefficient rapidly increases with changes in journal eccentricity for all operating eccentricities.

4 Increasing external pressurization decreases the extent of the cavitated region in the damper bearing. For a fully uncavitated bearing where the journal undergoes circular precession at constant eccentricity, the hydrodynamic stiffness disappears. However, the damping is twice that of the fully cavitated (180 deg film) bearing. If cavitation is prevented either a retainer spring or rotor preload must be employed as the bearing no longer has a unidirectional load carrying capacity.

5 Effective stiffness and damping coefficients can be calculated directly from rotating unbalance forces, rotor amplitude, and phase

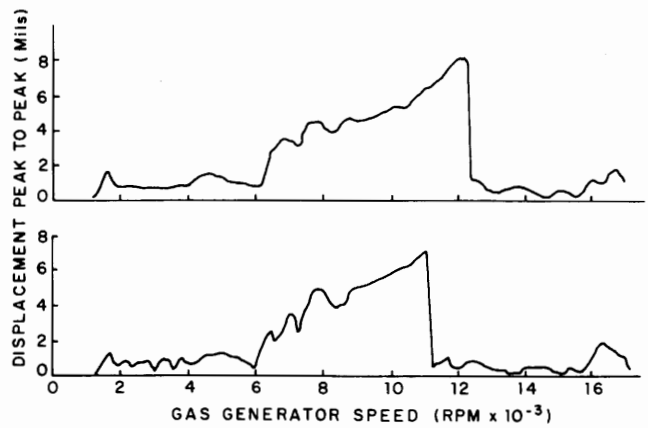

Fig. 11 Experimental amplitude of rotor mounted in squeeze film bearings showing nonlinear amplitude jump

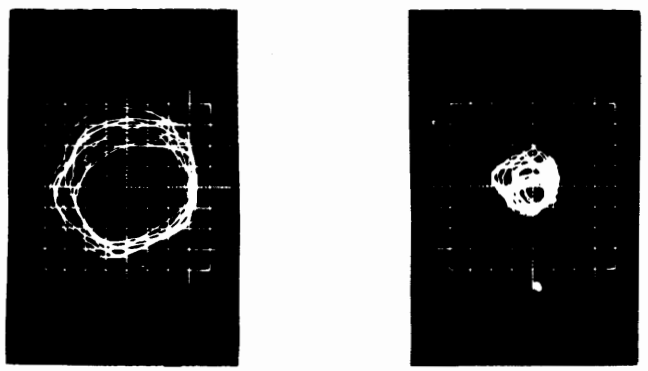

(a) (b)

Fig. 12 Experimental oscilloscope orbits of rotor mounted in squeeze film bearing showing nonlinear amplitude jump: (*a*) N = 16,500 rpm (*b*) N = 17,500 rpm

angle changes if the rotor acts as a rigid rotor in the operating speed range and its motion is approximately circular synchronous precession. For this case, the phase angle change of the journal (as measured by a timing mark or the journal in a damper) from low speed to operating speed must be approximately 120 deg opposite the direction of rotation for the dynamic transmissibility of the damper to be less than unity.

6 Time transient analyses of squeeze film bearings are necessary in damper design because circular synchronous precession of the journal about the bearing center is not always achieved and the linearized stiffness and damping coefficients no longer provide a valid description of the system. The damper pressure film extent in the transient analysis is not limited to 180 deg but is variable depending on the external pressure level.

7 The addition of retainer springs can have various effects:

a If the amplitude of the journal orbit is very large, the addition of retainer springs has little effect because the damper is generating a very large hydrodynamic stiffness.

b If the journal orbit remains in the lower half of the damper, the addition of retainer springs may help center the journal in the bearing and reduce the dynamic transmissibility. However, it is possible to operate a cavitated damper without retainer springs and produce a dynamic transmissibility less than 1.

c No instances of dynamic transmissibility less than 1 were observed in a fully cavitated damper, with or without retainer springs, when the unbalance eccentricity ratio, EMU, was ≥ 0.5.

8 Unidirectional loading causes an increase in the dynamic transmissibility and may also cause subharmonic whirl motion due to the nonlinear film effect (this subharmonic motion should not be confused with half-frequency oil whirl obtained in journal bearings). When the journal was centered by a preload force no instances of nonsynchronous motion were observed.

9 For a given damper bearing configuration there is an unbalance level above which the equilibrium operating eccentricity assumed by the rotor is bifurcated. This is often referred to as the "jump" phenomenon associated with nonlinear hardening springs in rotor systems. As the rotor speed is increased above the bifurcation point, the rotor assumes a large operating eccentricity and at a certain speed the eccentricity may "jump" to a lower value. When the speed is decreased, the rotor eccentricity will again "jump" to a higher value. This phenomenon has been observed in gas turbine engines employing squeeze film dampers under high unbalance conditions.

10 The incorporation of a squeeze film damper into an engine may result in an increase of transmitted forces above the rigid support value regardless of unbalance if the damper is operating in a speed range where $\omega/\omega_s < 1.4$. This region of operation should be avoided.

References

1 Lund, J. W., "Rotor-Bearing Design Technology—Part V," Technical Report AFAPL-TR-65-45, May 1965, Aero Propulsion Lab, Wright-Patterson Air Force Base, Dayton, Ohio.

2 Gunter, E. J., "Influence of Flexibly Mounted Rolling Element Bearings on Rotor Response—Part I—Linear Analysis," JOURNAL OF LUBRICATION TECHNOLOGY, TRANS. ASME, Jan. 1970, pp. 59–75.

3 Kirk, R. G., and Gunter, E. J., "The Effect of Support Flexibility and Damping on the Synchronous Response of a Single Mass Rotor," *Journal of Engineering for Industry*, TRANS. ASME, Feb. 1972, pp. 221–232.

4 Kirk, R. G., and Gunter, E. J., "Nonlinear Transient Analysis of Multimass Flexible Rotors—Theory and Applications," NASA CR-2300, Sept. 1973.

5 Cunningham, R. E., Fleming, D. P., and Gunter, E. J., "Design of a Squeeze Film Damper for a Multimass Flexible Rotor," *Journal of Engineering for Industry*, TRANS. ASME, Nov. 1975, pp. 1383–1389.

6 Barrett, L. E., and Gunter, E. J., "Steady-State and Transient Analysis of a Squeeze Film Damper Bearing for Rotor Stability," NASA CR-2548, May 1975.

7 Kirk, R. G., and Gunter, E. J., "Transient Journal Bearing Analysis," NASA CR-1549, June 1970.

8 McGrew, J. M., Discussion to reference [2].

9 Kirk, R. G., and Gunter, E. J., "Stability and Transient Motion of a Plain Journal Mounted in Flexible Damped Supports," ASME Paper No. 75-DET-116.

10 Mohan, S., and Hahn, E. J., "Design of Squeeze Film Damper Supports for Rigid Rotors," *Journal of Engineering for Industry*, TRANS. ASME, Aug. 1974, pp. 976–982.

Acknowledgment

The research described herein was supported in part by NASA Lewis Research Center, Contract No. NGL 47-005-050, under the supervision of Mr. William J. Anderson, Chief, Bearing Division and Mr. Robert E. Cunningham, Project Monitor whose support and encouragement is appreciated by the authors.